Electronic Supplementary Material (ESI) for Nanoscale.

Supporting Information

(Co, Mn)-doped $NiSe_2$- diethylenetriamine (dien) nanosheets and (Co, Mn, Sn)-doped $NiSe_2$ nanowires for high performance supercapacitor: compositional/morphological evolution and (Co, Mn)-induced electron transfer

Huamei Dan, Keyu Tao, Yang Hai, Li Liu and Yun Gong*

***Corresponding author: gongyun7211@cqu.edu.cn**

Table S1 The names of the samples synthesized under different conditions

	$Co(OAc)_2$ (mmol)	$Mn(OAc)_2$ (mmol)	Urea (mmol)	Selenization product
Co-precursor/NF	0.5	/	2.5	Co-$NiSe_2$-dien/NF
Co-Mn-precursor-2/NF	0.33	0.17	2.5	(Co, Mn)-$NiSe_2$-dien/NF
Co-Mn-precursor-1/NF	0.25	0.25	2.5	Co-$NiSe_2$-dien/$Mn(OH)_2$/NF
Co-Mn-precursor -0.5/NF	0.17	0.33	2.5	Co-$NiSe_2$-dien/$Mn(OH)_2$ /$MnCO_3$/NF
Mn-precursor/NF	/	0.5	2.5	$MnCO_3$/$NiSe_2$-dien/NF
Bare Ni foam	/	/	/	$NiSe_2$-dien/NF

(a)

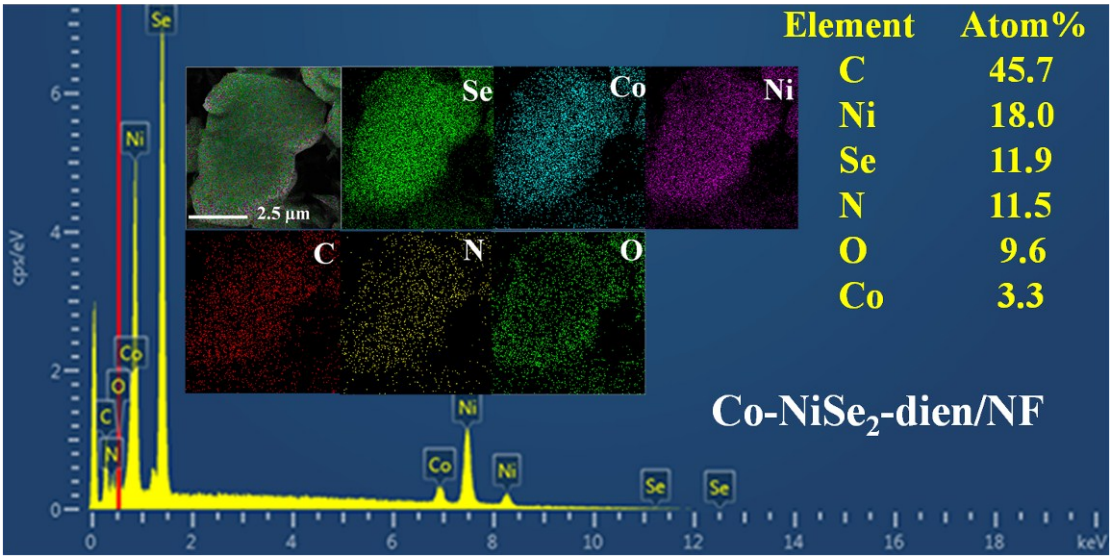

(b)

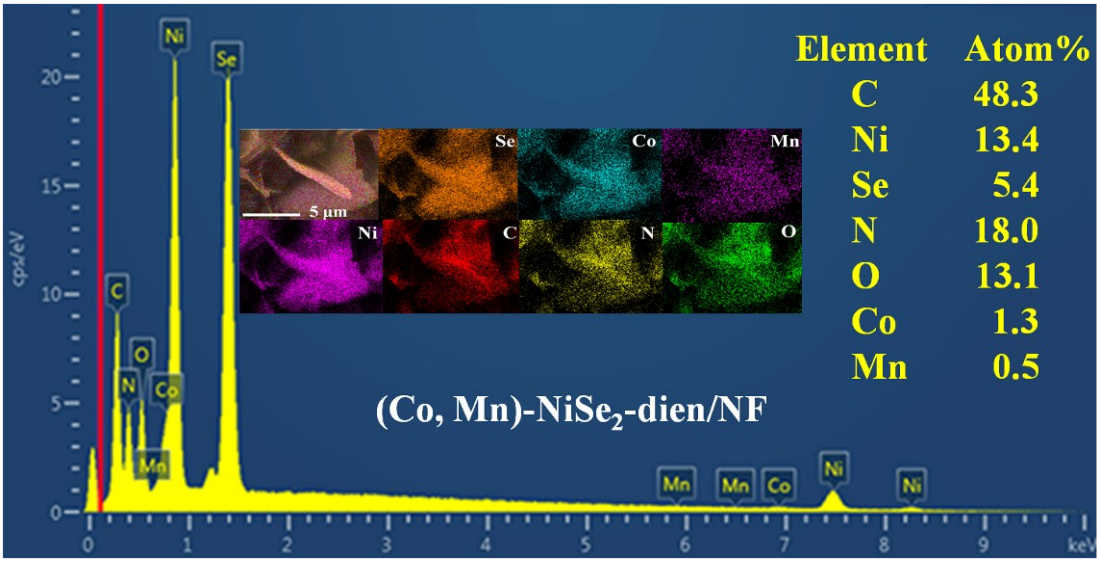

(c)

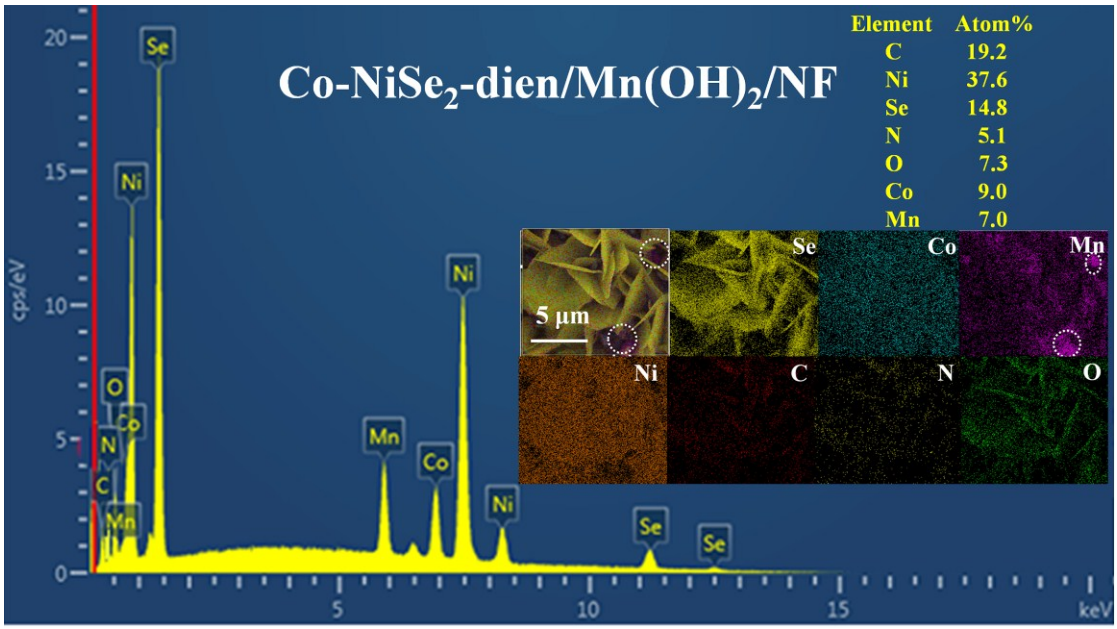
Co-NiSe2-dien/Mn(OH)2/NF
Element Atom%
C 19.2
Ni 37.6
Se 14.8
N 5.1
O 7.3
Co 9.0
Mn 7.0
5 μm
Se
Co
Mn
Ni
C
N
O
cps/eV
keV

(d)

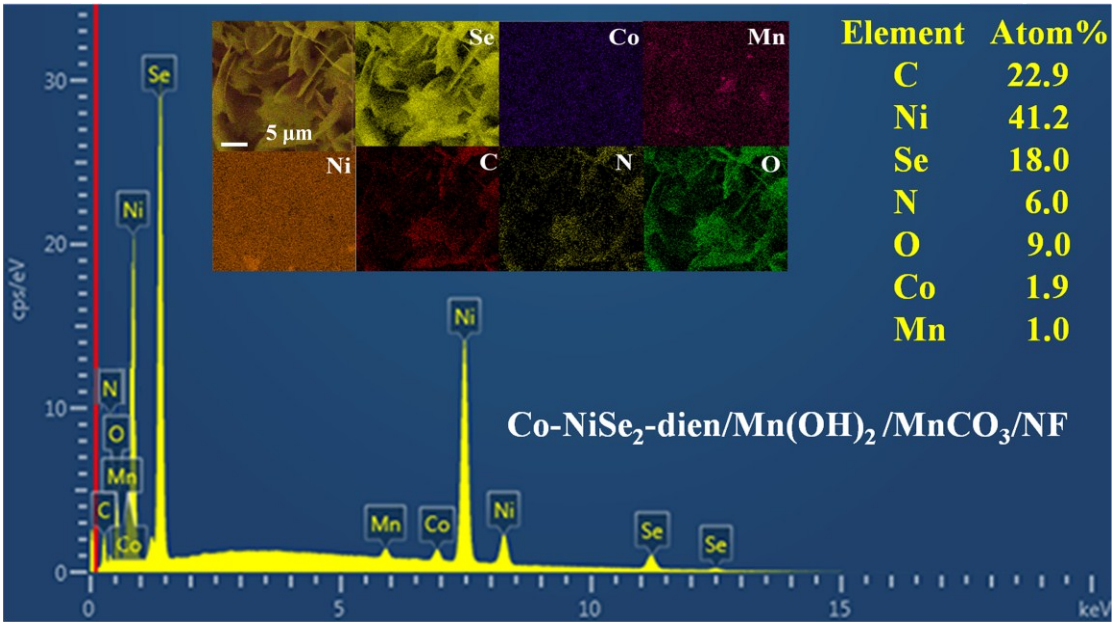
Element Atom%
C 22.9
Ni 41.2
Se 18.0
N 6.0
O 9.0
Co 1.9
Mn 1.0
5 μm
Co-NiSe2-dien/Mn(OH)2 /MnCO3/NF
cps/eV
keV

(e)

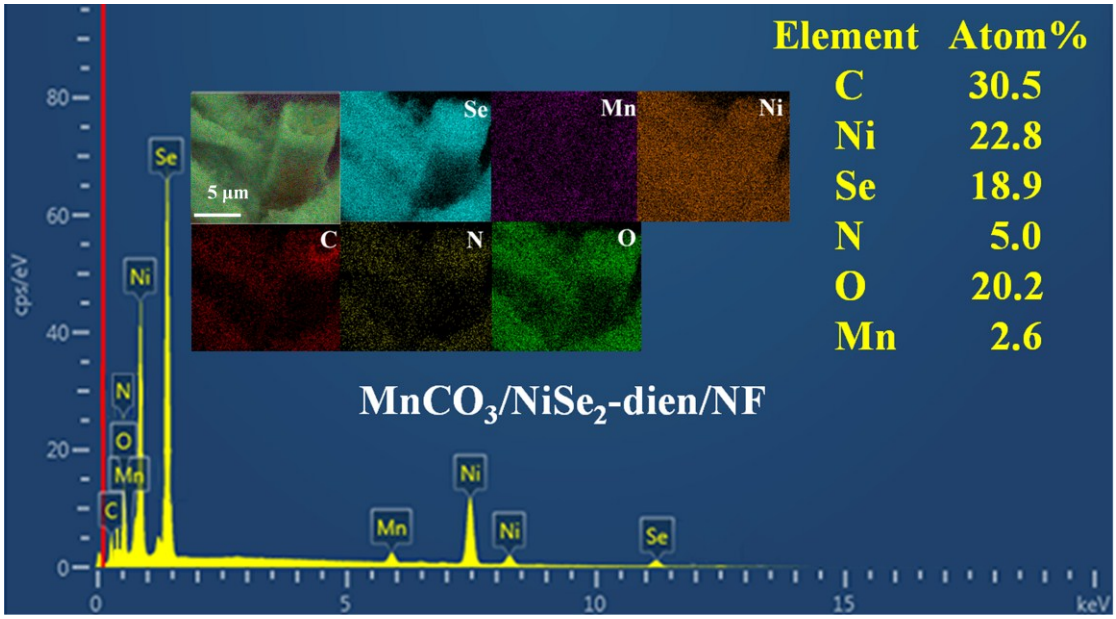

Figure S1 EDS and elemental mappings (inset) of (**a**) Co-$NiSe_2$-dien/NF, (**b**) (Co, Mn)-$NiSe_2$-dien/NF, (**c**) Co-$NiSe_2$-dien/$Mn(OH)_2$/NF, (**d**) Co-$NiSe_2$-dien/$Mn(OH)_2$ /$MnCO_3$/NF and (**e**) $MnCO_3$/ $NiSe_2$-dien/NF.

Table S2 The atomic percentages (at. %) for all the selenization samples

Sample	Co -$NiSe_2$ -dien/NF	(Co, Mn) -$NiSe_2$ -dien /NF	Co-$NiSe_2$-dien /$Mn(OH)_2$ /NF	Co-$NiSe_2$-dien /$Mn(OH)_2$ /$MnCO_3$/ NF	$MnCO_3$/ $NiSe_2$-dien/NF	$NiSe_2$ -dien/NF	(Co, Mn) -$NiSe_2$ -dien /NF after cycling test
Co	3.3	1.3	9.0	1.9	/	/	2.3
Mn	/	0.5	7.0	1.0	2.6	/	0.0
Ni	18.0	13.4	37.6	41.2	22.8	27.4	25.2
Se	11.9	5.4	14.8	18.0	18.9	15.6	0.0
C	45.7	48.3	19.2	22.9	30.5	35.9	22.8
N	11.5	18.0	5.1	6.0	5.0	6.7	0.0

O	9.6	13.1	7.3	9.0	20.2	14.4	49.4

(a) **(b)**

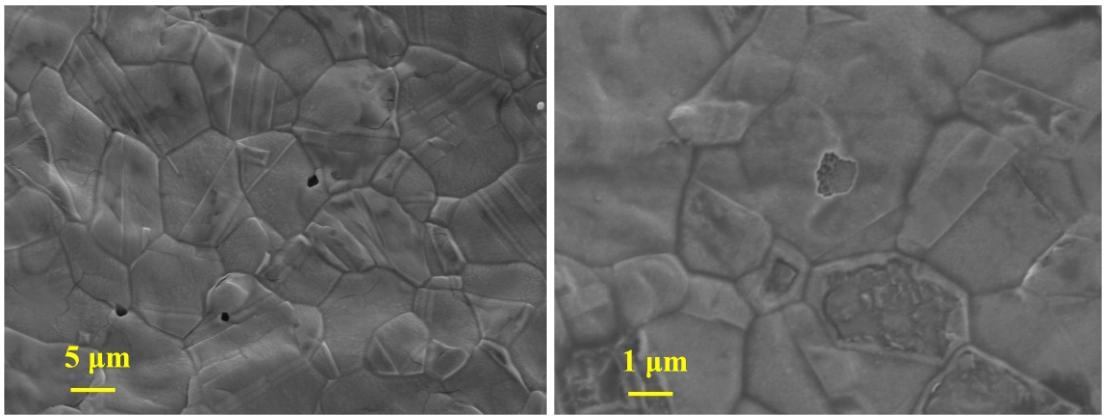

(c)

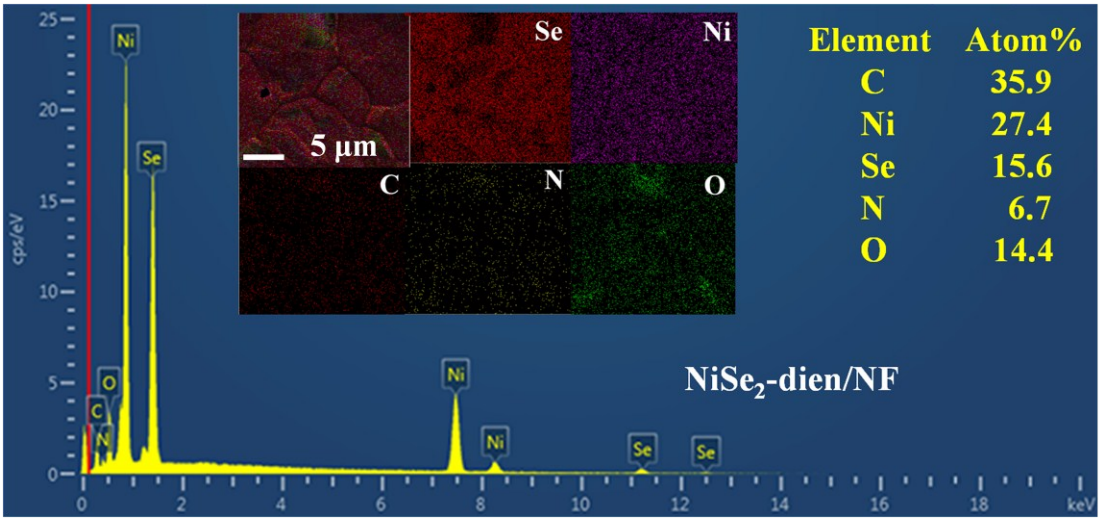

Figure S2 (**a, b**) SEM and (**c**) EDS images as well as elemental mappings (inset) of $NiSe_2$-dien/NF.

(a)

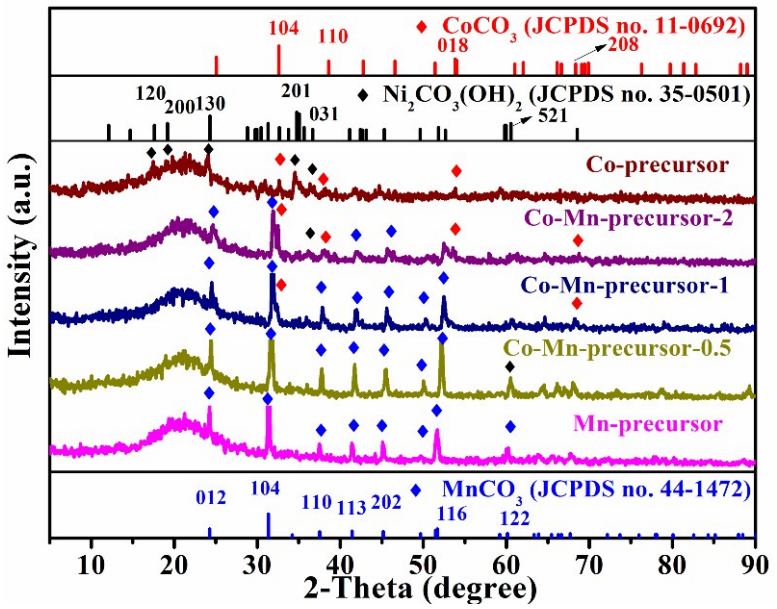

(b)

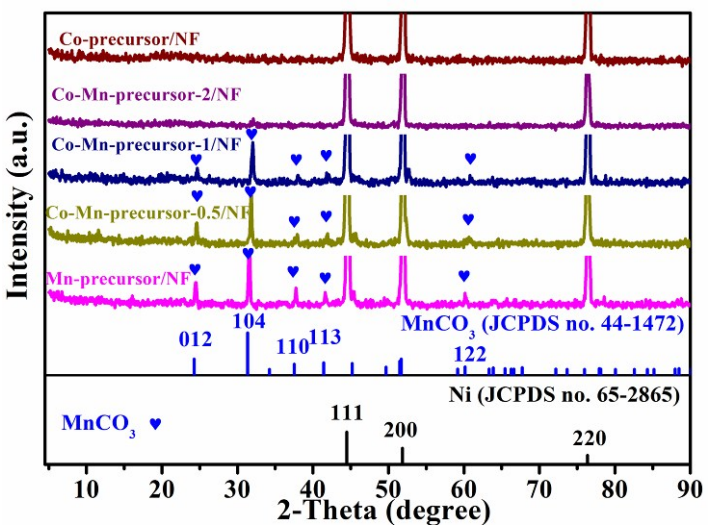

Figure S3 XRD patterns of (**a**) precipitations and (b) precursors grown on Ni foam.

(a) **(b)**

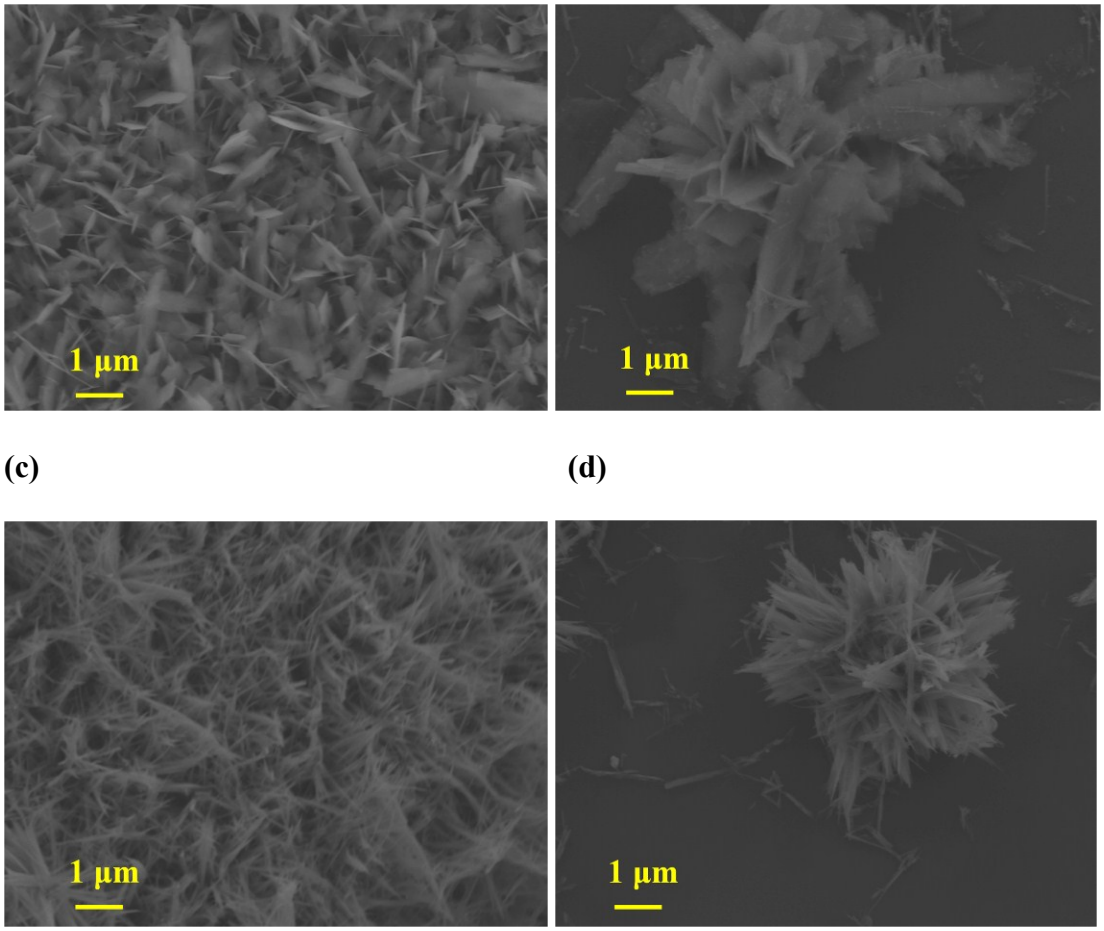

Figure S4 SEM images of (**a**) Co-precursor/NF, (**b**) Co-precursor precipitation, (**c**) Co-Mn-precursor-2/NF and (**d**) Co-Mn-precursor-2 precipitation.

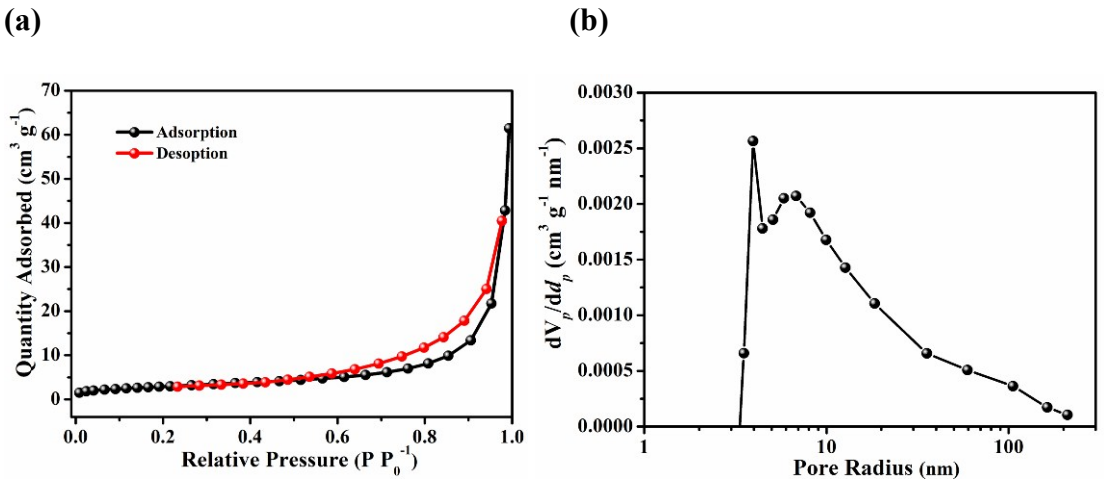

Figure S5 (**a**) Nitrogen adsorption-desorption isotherms and (**b**) the corresponding pore-size distribution curve of (Co, Mn)-$NiSe_2$-dien/NF.

Table S3 (**a**) The electrochemical performances of (Co, Mn)-$NiSe_2$-dien/NF and other electrode materials.

	Electrode material (three-electrode cell)	Specific capacity	Current density	Electrolyte	Ref.
1	α-MnSe	96.76 F g^{-1}	0.1 mA cm^{-2}	1 M Li_2SO_4	1
2	$Co_{0.85}Se$	294 F g^{-1}	0.5 A g^{-1}	2 M KOH	2
3	$Co_{0.85}Se@MoSe_2$	774 F g^{-1}	1 A g^{-1}	2 M KOH	3
4	$CoSe@MoSe_2$	128.2 mAh g^{-1}	1 A g^{-1}	2 M KOH	4
5	$(Ni_{0.33}Co_{0.67})Se_2$	827.9 F g^{-1}	1 A g^{-1}	3 M KOH	5
6	$Co_{0.85}Se$	114.6 mAh g^{-1}	1 A g^{-1}	2 M KOH	6
7	$Ni_{0.6}Co_{0.4}Se_2$//AC	1580 F g^{-1}	1 A g^{-1}	2 M KOH	7
8	$Cu_{0.63}Co_{0.37}Se_2$	28.63 F g^{-1}	1 A g^{-1}	2 M KOH	8
9	$Co_{0.85}Se$	422 F g^{-1}	1 A g^{-1}	2 M KOH	9
10	CoSe	70.6 mAh g^{-1}	1 A g^{-1}	2 M KOH	10
11	$Ni_{0.9}Co_{1.92}Se_4$ @MnO_2	1021.1F g^{-1}	2 mA cm^{-2}	3 M KOH	11
12	CoSe	544.6 F g^{-1}	1 mA cm^{-2}	3 M KOH	12
13	MnCo-LDH@$Ni(OH)_2$	2320 F g^{-1}	3 A g^{-1}	3 M KOH	13
14	Mn-Co-Fe HNPs	1170 F g^{-1}	2 A g^{-1}	6 M KOH	14
15	$MnCO_3@MnO_2$	363 F g^{-1}	1 A g^{-1}	1 M Na_2SO_4	15
16	$Ni_{0.2}Mn_{0.8}CO_3$	583.5 F g^{-1}	1 A g^{-1}	3 M KOH	16
17	CuS	237 F g^{-1}	0.5 A g^{-1}	2 M KOH	17

18	CoO/Co_3O_4	451 F g^{-1}	1 A g^{-1}	3 M KOH	18
19	CWS/Ni	2666.6 F g^{-1}	10 mA cm^{-2}	1 M Li_2SO_4	19
20	PB@MnO2	608 F g^{-1}	1 A g^{-1}	1 M KNO_3	20
21	$K_{0.27}MnO_2 \cdot 0.6H_2O$	144.7 F g^{-1}	2 C	0.5 M K_2SO_4	21
22	Cu_3SbS_4/Ni-5	835.24 mAh g^{-1}	2.5 mA cm^{-2}	1 M LiOH	22
23	**(Co, Mn)-$NiSe_2$-dien /NF**	**288.6 mAh g^{-1}**	**1 A g^{-1}**	**2 M KOH**	**This work**

Table S3(b) comparisons of (Co, Mn)-$NiSe_2$-dien/NF//AC device with other two-elelctrode devices reported in literatures.

	Device (two-electrode cell)	Energy density	Electrolyte	Capacity retention	Ref.
1	α-MnSe//α-MnSe	2.08 Wh kg^{-1} at 25 W kg^{-1}	1 M Li_2SO_4	103.4 % (2000 cycles at 2 mA cm^{-2})	1
2	$Co_{0.85}Se$//N-PCNs	21.1 Wh kg^{-1} at 400 W kg^{-1}	2 M KOH	93.8 % (5000 cycles)	2
3	$Co_{0.85}Se$@$MoSe_2$//GNS	25.5 Wh kg^{-1} at 420 W kg^{-1}	2 M KOH	88 % (5000 cycles at 10 A g^{-1})	3
4	CoSe@$MoSe_2$//N-PMCN	32.6 Wh kg^{-1} at 415 W kg^{-1}	2 M KOH	91.4 % (5000 cycles at 5 A g^{-1})	4
5	$(Ni_{0.33}Co_{0.67})Se_2$//AC	29.1 Wh kg^{-1} at 800 W kg^{-1}	3 M KOH	113 % (2000 cycles at 6 A g^{-1})	5
6	$Co_{0.85}Se$//AC	22.3 Wh kg^{-1} at 829 W kg^{-1}	2 M KOH	76 % (5000 cycles at 5 A g^{-1})	6
7	$Ni_{0.6}Co_{0.4}Se_2$//AC	44.1 Wh kg^{-1} at 691.3 kW kg^{-1}	2 M KOH	89.2 % (20000 cycles at 10 A g^{-1})	7
8	$Cu_{0.63}Co_{0.37}Se_2$//AC	0.192 Wh kg^{-1} at 36.65 W kg^{-1}	2 M KOH	96.5 % (2000 cycles at 1 A g^{-1})	8
9	$Co_{0.85}Se$//AC	17.8 Wh kg^{-1} at	2 M KOH	93 % (2000 cycles at	9

		3.57 kW kg^{-1}		1A g^{-1})	
10	CoSe//AC	18.6 W h kg^{-1} at 750 W kg^{-1}	2 M KOH	95.4 % (20000 cycles at 5 A g^{-1})	10
11	$Ni_{0.9}Co_{1.92}Se_4$ @MnO_2//AC	26.29 W h kg^{-1} at 265 W kg^{-1}	3 M KOH	88.39 % (5000 cycles at 20 mA cm^{-2})	11
12	CoSe//AC	20.2 W h kg^{-1} at 144.1 W kg^{-1}	3 M KOH	93.3 % (5000 cycles at 10 mA cm^{-2})	12
13	MnCo-LDH@$Ni(OH)_2$//AC	47.9 W h kg^{-1} at 750.7 W kg^{-1}	3 M KOH	90.9 % (5000 cycles at 20 A g^{-1})	13
14	Mn-Co-Fe HNPs//AC	11.4 W h kg^{-1} at 1125 W kg^{-1}	6 M KOH	96 % (4000 cycles at 5 A g^{-1})	14
15	$MnCO_3$@MnO_2//AG	27.4 W h kg^{-1} at 271.7 W kg^{-1}	1 M Na_2SO_4	84.2 % (2000 cycles at 1 A g^{-1})	15
16	$Ni_{0.2}Mn_{0.8}CO_3$//AC	24.1 W h kg^{-1} at 740 W kg^{-1}	3 M KOH	84.8 % (2000 cycles at 2 A g^{-1})	16
17	CuS//AC	15.1 W h kg^{-1} at 392.9 W kg^{-1}	2 M KOH	88 % (4000 cycles at 1 A g^{-1})	17
18	CoO/Co_3O_4//AC	10.52 W h kg^{-1} at 140 W kg^{-1}	3 M KOH	_____	18
19	CWS/Ni//graphene	48.6 W h kg^{-1} at 321.4 W kg^{-1}	1 M Li_2SO_4	92.1% (10000 cycles)	19
20	PB@MnO2//PG	16.5 W h kg^{-1} at 550 W kg^{-1}	1 M KNO_3	93% (4000 cycles at 1 A g^{-1})	20
21	$K_{0.27}MnO_2 \cdot 0.6H_2O$// AC	25.3 W h kg^{-1} at 140 W kg^{-1}	0.5 M K_2SO_4	98% (10000 cycles at 25C)	21
22	Cu_3SbS_4/Ni-5//Cu_2MoS_4/Ni	58.15 W h kg^{-1} at 636.4 W kg^{-1}	1 M LiOH	96.7% (1000 cycles at 15 mA cm^{-2})	22
23	**(Co, Mn)-$NiSe_2$-dien /NF//AC**	**50.94 Wh kg^{-1} at 447.3 W kg^{-1}**	**2 M KOH**	**84 % (10000 cycles at 8 A g^{-1})**	**This work**

Table S4 The values of the parameters in the equivalent circuits for (Co, Mn)-$NiSe_2$-dien/NF (before and after 10000 GCD cycles), Co-$NiSe_2$-dien/NF, $NiSe_2$-dien/NF and

(Co,Mn)-$NiSe_2$-dien/NF//AC device.

Electrode	R_s/Ω cm^{-2}	C/F cm^{-2}	R_{ct}/Ω cm^{-2}	W/Ω cm^{-2}
(Co, Mn)-$NiSe_2$-dien/NF before 10000 GCD cycles	0.853	0.581	39.2	0.1172
(Co, Mn)-$NiSe_2$-dien/NF after 10000 GCD cycles	1.059	0.3577	86.2	0.0487
Co-$NiSe_2$-dien/NF	1.207	0.0152	527	0.0098
$NiSe_2$-dien/NF	1.843	0.0087	1376	0.0048
(Co,Mn)-$NiSe_2$-dien/NF//AC device	1.848	0.4203	108.7	0.1683

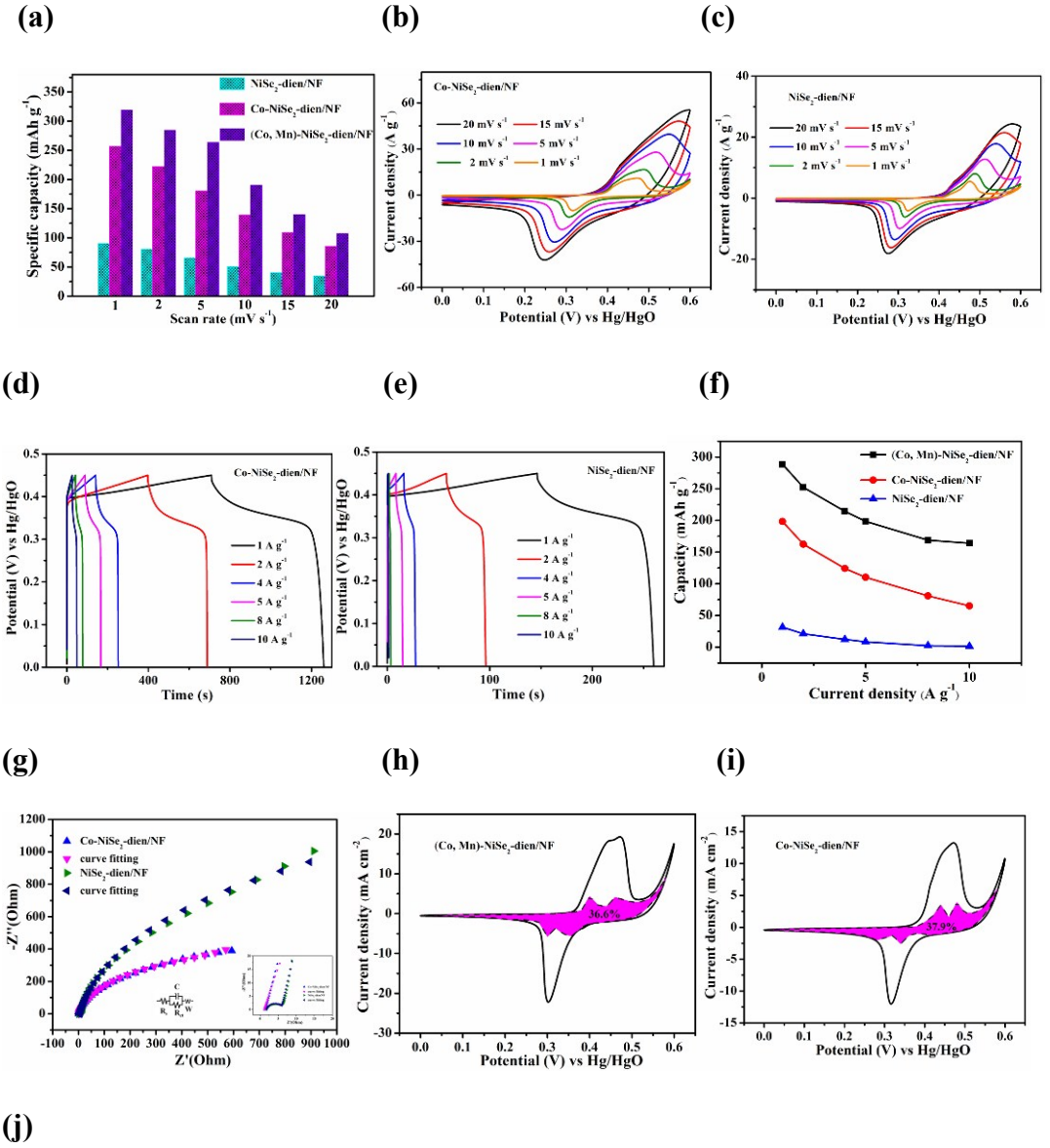

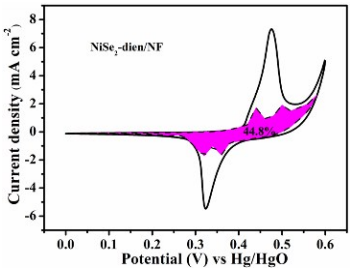

Figure S6 (**a, f**) The comparisons of specific capacities at (**a**) different scan rates and (**f**) different current densities; (**b, c**) CVs at different scan rates and (**d, e**) GCD curves at different current densities of (**b, d**) Co-$NiSe_2$-dien/NF and (**c, e**) $NiSe_2$-dien/NF; (**g**) Nyquist plots; CVs at 1 mV s^{-1} of (**h**) (Co, Mn)-$NiSe_2$-dien/NF, (**i**) Co-$NiSe_2$-dien/NF and (**j**) $NiSe_2$-dien/NF, in which the surface capacities are highlighted in shaded regions.

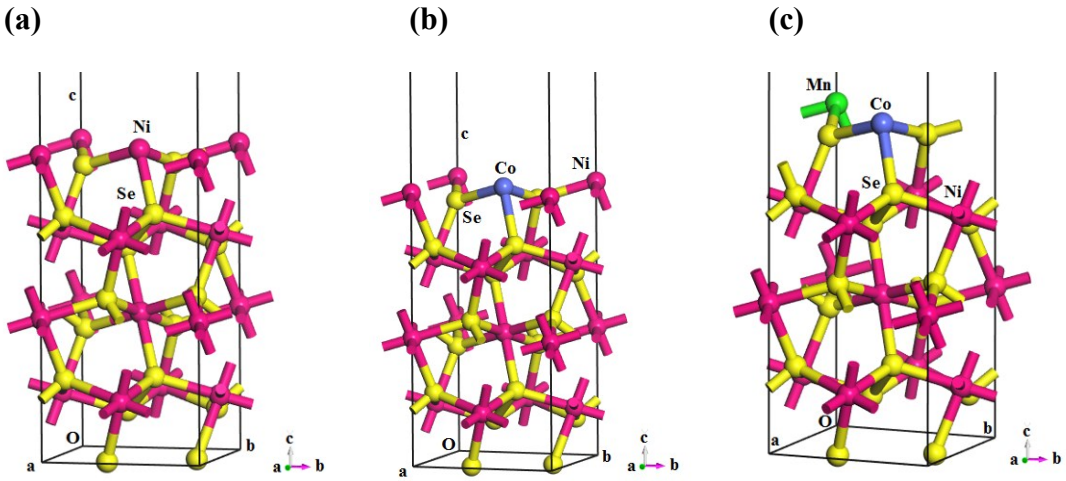

Figure S7 The models for (**a**) $NiSe_2$, (**b**) Co-substituted $NiSe_2$ and (**c**) (Co, Mn)-substituted $NiSe_2$. Color codes: pink, Ni; yellow, Se; blue, Co; green, Mn.

(a)

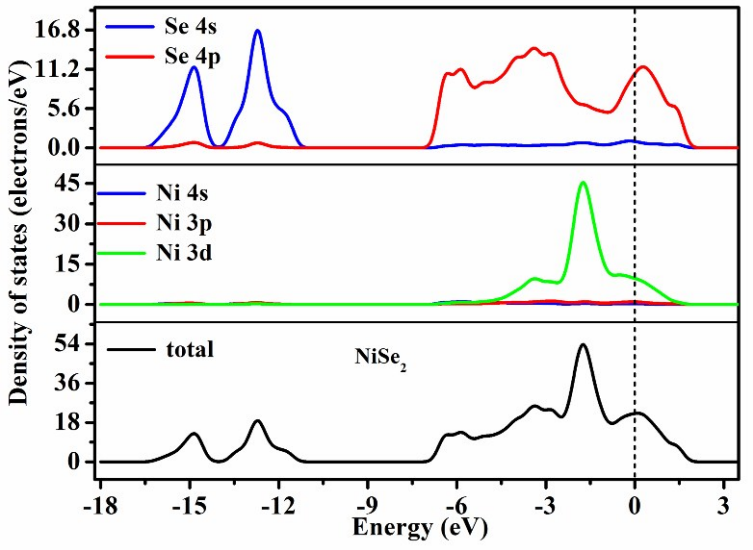
Se 4s
Se 4p
Ni 4s
Ni 3p
Ni 3d
total
NiSe2
Density of states (electrons/eV)
Energy (eV)

(b)

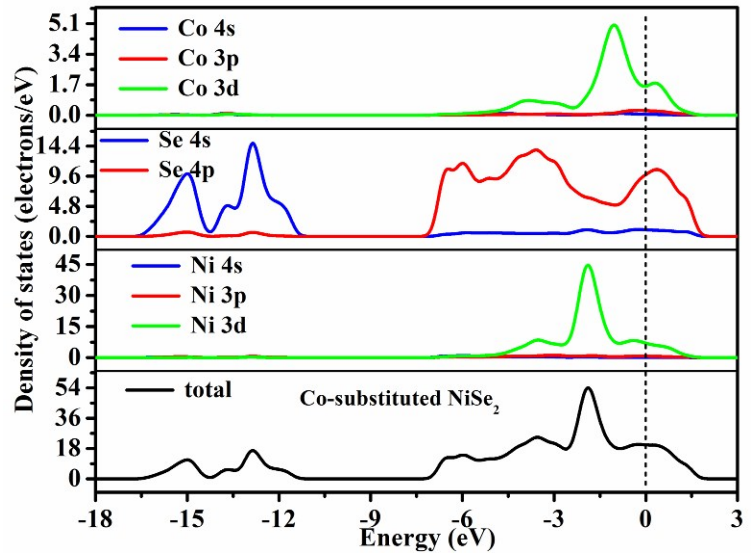
Co 4s
Co 3p
Co 3d
Se 4s
Se 4p
Ni 4s
Ni 3p
Ni 3d
total
Co-substituted NiSe2
Density of states (electrons/eV)
Energy (eV)

(c)

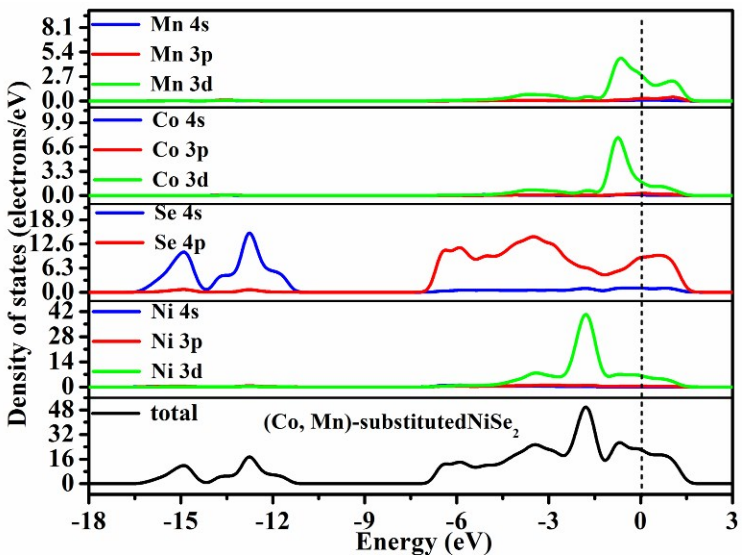

Figure S8 Total DOS (TDOS) and partial DOS (PDOS) of (**a**) $NiSe_2$, (**b**) Co-substituted $NiSe_2$ and (**c**) (Co, Mn)-substituted $NiSe_2$. Color codes: blue, s orbit; red, p orbit; green, d orbit.

(a) **(b)**

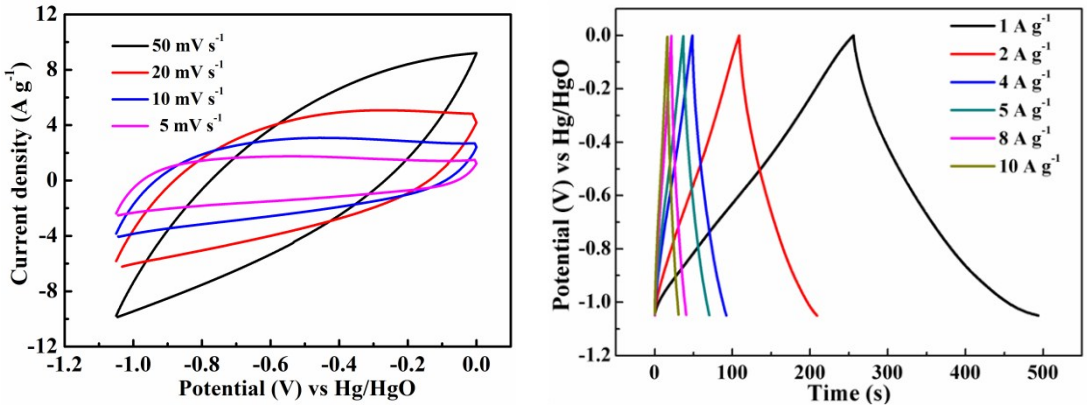

(c) **(d)**

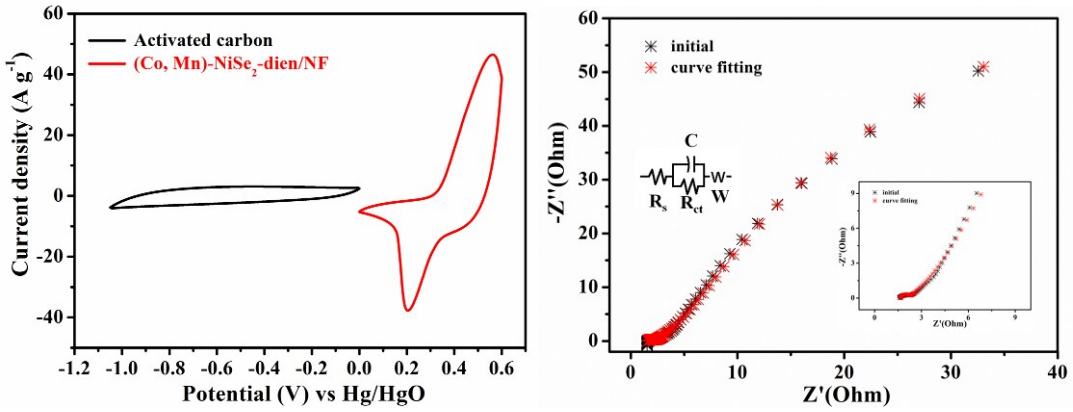

Figure S9 (**a**) CV curves at different scan rates and (**b**) GCD curves at different current densities of activated carbon (AC) in a three-electrode cell, (**c**) The comparative CV curves of the individual AC and (Co, Mn)-$NiSe_2$-dien/NF at 10 mV s^{-1}, (**d**) Nyquist plot for (Co, Mn)-$NiSe_2$-dien/NF//AC device.

(a) **(b)**

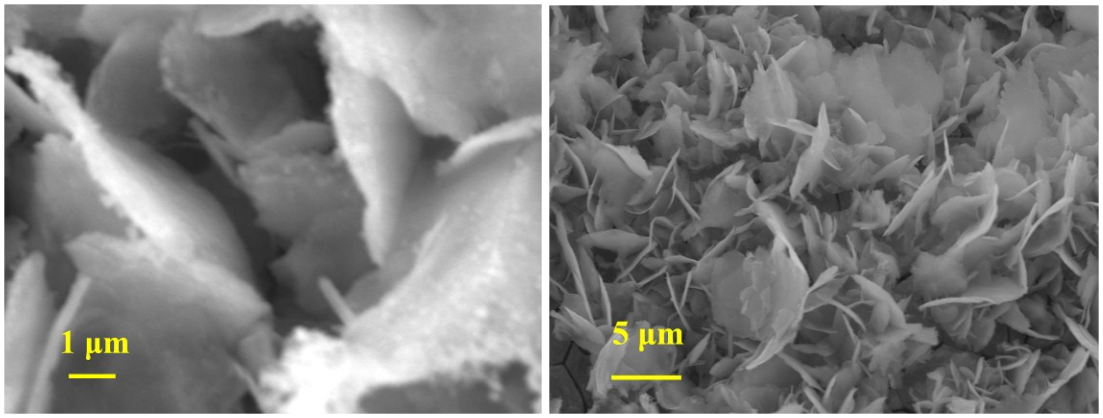

(c)

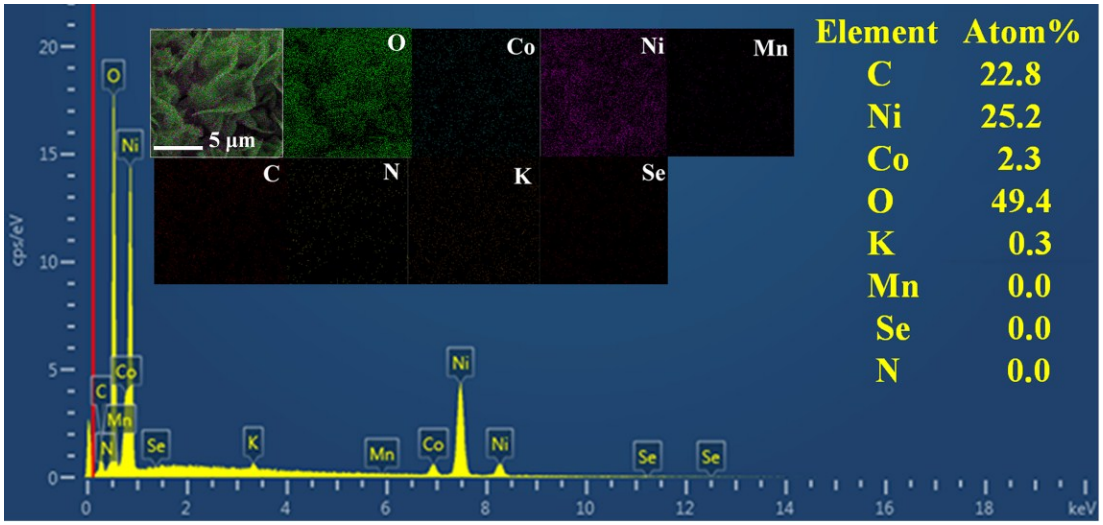

Figure S10 (**a, b**) SEM images and (**c**) EDS as well as the corresponding elemental mappings (**inset**) for (Co, Mn)-$NiSe_2$-dien/NF after 10000 GCD cycles.

(a)

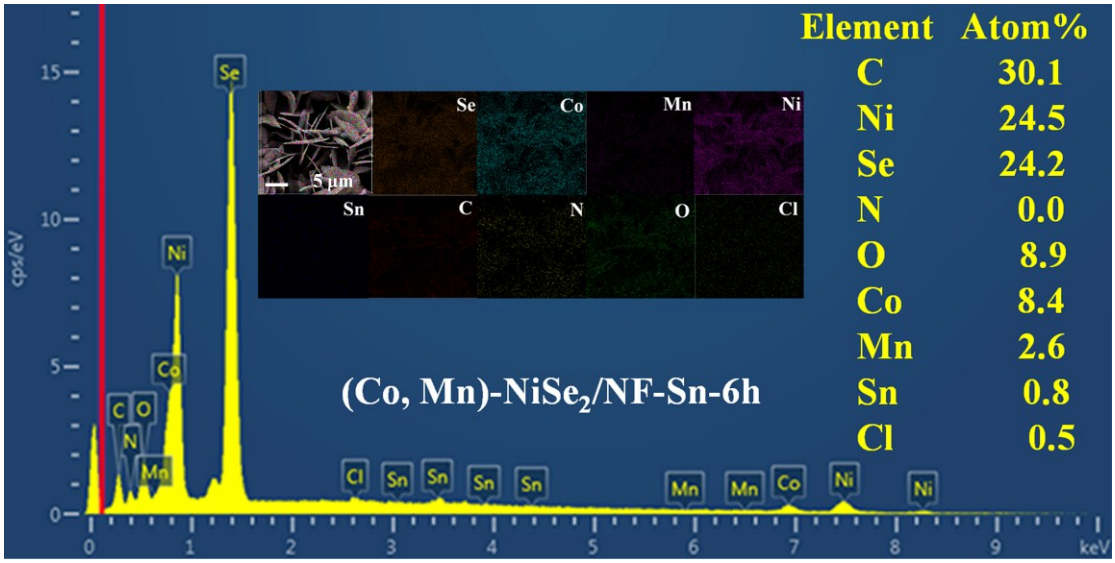

(b)

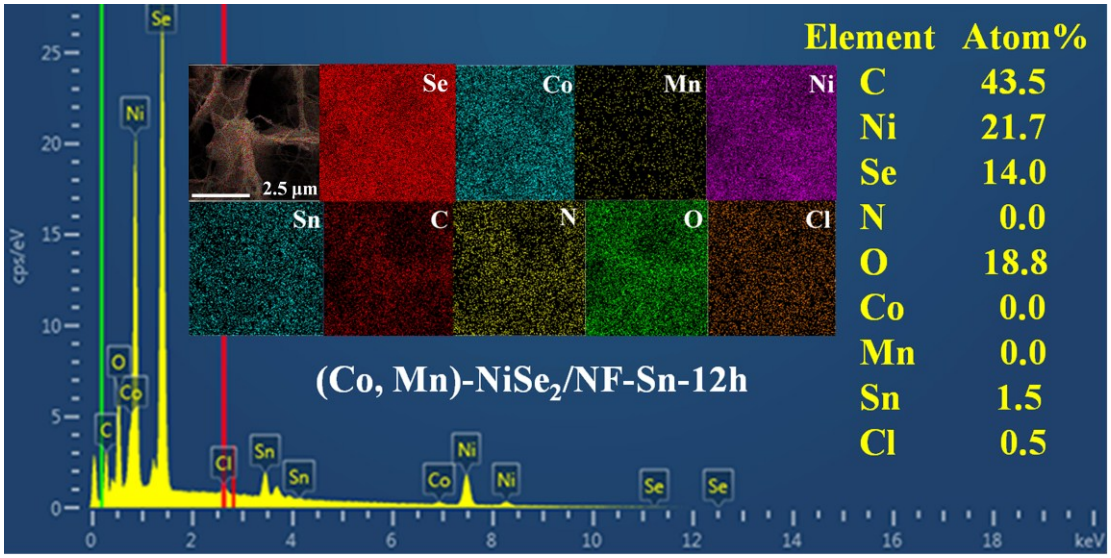

Figure S11 EDS images and elemental mappings (inset) of (**a**) (Co, Mn)-$NiSe_2$/NF-Sn-6h and (**b**) (Co, Mn)-$NiSe_2$/NF-Sn-12h.

References:

1 S. Sahoo, P. Pazhamalai, K. Krishnamoorthy and S. J. Kim, *Electrochim. Acta*, 2018, **268**, 403-410.

2 H. Peng, G. Ma, K. Sun, Z. Zhang, J. Li, X. Zhou and Z. Lei, *J. Power Sources*, 2015, **297**, 351-358.

3 H. Peng, C. Wei, K. Wang, T. Meng, G. Ma, Z. Lei and X. Gong, *ACS Appl. Mater. Interfaces*, 2017, **9**, 17067-17075.

4 H. Peng, J. Zhou, K. Sun, G. Ma, Z. Zhang, E. Feng and Z. Lei, *ACS Sustain. Chem. Eng*, 2017, **5**, 5951-5963.

5 L. Quan, T. Liu, M. Yi, Q. Chen, D. Cai and H. Zhan, *Electrochim. Acta*, 2018, **281**, 109-116.

6 S. Wu, Q. Hu, L. Wu, J. Li, H. Peng and Q. Yang, *J. Alloys Compd.*, 2019, **784**, 347-353.

7 S. Xie, J. Gou, B. Liu and C. Liu, *J. Colloid Interface Sci.*, 2019, **540**, 306-314.

8 B. K. Deka, A. Hazarika, J. Kim, N. Kim, H. E. Jeong, Y. B. Park and H. W. Park, *Chem. Eng. J.*, 2019, **355**, 551-559.

9 X. Zhao, X. Li, Y. Zhao, Z. Su, Y. zhang and R. Wang, *J. Alloys Compd.*, 2017, **697**, 124-131.

10 Y. Zhu, Z. Huang, Z. Hu, L. Xi, X. Ji and Y. Liu, *Electrochim. Acta*, 2018, **269**, 30-37.

11 W. An, L. Liu, Y. Gao, Y. Liu and J. Liu, *RSC Adv.*, 2016, **6**, 75251-75257.

12 T. Chen, S. Li, P. Gui, J. Wen, X. Fu and G. Fang, *Nanotechnology*, 2018, **29**, 205401.

13 S. Liu, S. C. Lee, U. Patil, I. Shackery, S. Kang, K. Zhang, J. H. Park, K. Y. Chung and S. Chan Jun, *J. Mater. Chem. A*, 2017, **5**, 1043-1049.
14 A. E. Elkholy, F. El Taib Heakal and N. K. Allam, *Electrochim. Acta*, 2019, **296**, 59-68.
15 H. Chen, Z. Yan, X. Y. Liu, X. L. Guo, Y. X. Zhang and Z. H. Liu, *J. Power Sources*, 2017, **353**, 202-209.
16 N. Zhao, H. Fan, M. Zhang, X. Ren, C. Wang, H. Peng, H. Li, X. Jiang and X. Cao, *Ceram. Int.*, 2019, **45**, 5266-5275.
17 J. Zhang, H. Feng, J. Yang, Q. Qin, H. Fan, C. Wei and W. Zheng, *ACS Appl. Mater. Interfaces*, 2015, **7**, 21735-21744.
18 M. Pang, G. Long, S. Jiang, Y. Ji, W. Han, B. Wang, X. Liu, Y. Xi, D. Wang and F. Xu, *Chem. Eng. J.*, 2015, **280**, 377-384.
19 P. Pazhamalai, K. Krishnamoorthy, S. Sahoo, V. K. Mariappan and S. J. Kim, *Chem. Eng. J.*, 2019, **359**, 409-418.
20 A. K. Das, R. Bera, A. Maitra, S. K. Karan, S. Paria, L. Halder, S. K. Si, A. Bera and B. B. Khatua, *J. Mater. Chem. A*, 2017, **5**, 22242-22254.
21 Q. Qu, L. Li, S. Tian, W. Guo, Y. Wu and R. Holze, *J. Power Sources*, 2010, **195**, 2789-2794.
22 V. K. Mariappan, K. Krishnamoorthy, P. Pazhamalai, S. Sahoo, S. S. Nardekar and S. J. Kim, *Nano Energy*, 2019, **57**, 307-316.